A Tunable Broadband Photonic RF Phase Shifter Based on a Silicon Microring Resonator

Qingjiang Chang, *Student Member, IEEE*, Qiang Li, *Student Member, IEEE*, Ziyang Zhang, Min Qiu, *Member, IEEE*, Tong Ye, and Yikai Su, *Senior Member, IEEE*

***Abstract*—We propose and demonstrate a tunable broadband photonic radio frequency (RF) phase shifter based on a silicon microring resonator. This scheme utilizes the thermal nonlinear effect of the silicon microring to change the electrical phase of the RF signal with a wide tuning range. A prototype of the phase shifter is experimentally demonstrated for a 40-GHz signal with a 0-4.6-rad tuning range.**

***Index Terms*—Microwave photonics, photonic radio frequency (RF) phase shifter, silicon microring resonator.**

I. Introduction

RADIO frequency (RF) phase shifters have been playing an increasingly important role in phased-array beamforming systems and smart antenna applications. Conventional RF phase shifters have limitations in terms of operational bandwidth and phase-shift tuning range. Recently, the use of photonic elements to control the phase shift has raised attention due to the advantages of flexible tunability, high bandwidth, and light weight offered by optical systems [1]. Various techniques for realizing photonic RF phase shifters have been reported, including wavelength conversion in a distributed feedback laser (DFB) [2], stimulated Brillouin scattering (SBS) signal processing [3], homodyne mixing [4], and vector sum methods [5]. However, a practical implementation of phase arrays with thousands of elements is limited by the size and complexity of the conventional phase-shifting schemes. The use of miniaturized and integrated on-chip devices to perform this function is thus of much interest. Recently, we have concept-proved a photonic microwave phase shifter using a silicon microring resonator with preliminary demonstration, providing a 0-4.6-rad phase-shift tuning range for a 20-GHz signal [6]. In this letter, a 40-GHz tunable photonic RF phase shifter is presented and experimentally demonstrated. The maximum achievable phase shift versus the RF frequency, the power variation when varying the phase shift, and the response speed of the phase shift are further investigated. The proposed scheme is based on a 20-μm-radius silicon microring resonator, which features broadband operation, large phase-shifting range, reduced complexity, compact footprint size, and easy integration.

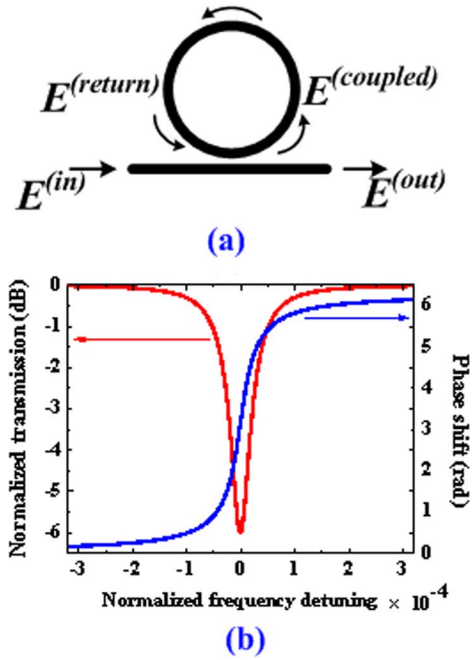

Fig. 1. (a) Basic structure of a single microring resonator. (b) Corresponding transmission spectrum and phase shift curve.

II. Principle

For a single-side coupled microring resonator, shown in Fig. 1(a), the linear transfer function can be expressed as [7]

$$T(\omega) = \frac{r - a\exp(j\phi)}{1 - ra\exp(j\phi)} \tag{1}$$

where r is the transmission coefficient and $a = \exp(-\alpha L/2)$ represents the single pass attenuation in the ring, where L and α are the length and the linear loss of the ring, respectively. $\phi = kL$ is the linear phase shift of the ring and k is the propagation constant. The total transmission phase-shift of the output field (E_{out}) is

$$\Delta\phi = \arctan\frac{ra\sin(\phi)}{1 - ra\cos(\phi)} - \arctan\frac{a\sin(\phi)}{r - a\cos(\phi)} \tag{2}$$

Manuscript received July 22, 2008; revised October 14, 2008. First published October 31, 2008; current version published January 05, 2009. This work was supported in part by the NSFC (60777040), in part by the 863 High-Tech Program (2006AA01Z255), in part by the Shanghai Rising Star Program Phase II (07QH14008), in part by the Swedish Foundation for Strategic Research (SSF) through the Future Research Leader Program, and in part by the Swedish Research Council (VR).

Q. Chang, Q. Li, T. Ye, and Y. Su are with the State Key Laboratory of Advanced Optical Communication Systems and Networks, Department of Electronic Engineering, Shanghai Jiao Tong University, Shanghai 200240, China (e-mail: yikaisu@sjtu.edu.cn).

Z. Zhang and M. Qiu are with the Department of Microelectronics and Applied Physics, Royal Institute of Technology, Electrum 229, 16440 Kista, Sweden.

Color versions of one or more of the figures in this letter are available online at http://ieeexplore.ieee.org.

Digital Object Identifier 10.1109/LPT.2008.2008658

which is largely dependent on the single-pass phase shift near resonance. Fig. 1(b) shows the transmission spectrum and the phase shift for a ring resonator with a 3-dB resonance bandwidth of 0.1 nm and a resonance notch depth of 6 dB. It depicts that a phase shift of π rad is achieved on resonance and the full phase shift tuning range is 0–2π rad.

To demonstrate a broadband photonic RF phase shifter, we employ optical carrier suppression (OCS) technology [8] to generate an optical millimeter wave with two tones of 40-GHz frequency spacing. The output field of the OCS signal driven by an RF signal $\cos(\omega_{\rm RF}t)$ can be expressed by

$$E_{\rm in}(t) = A_{-1}\exp[j(\omega_s - \omega_{\rm RF})t] + A_1\exp[j(\omega_s + \omega_{\rm RF})t] \tag{3}$$

where A_{-1} and A_1 are the amplitudes of the two tones of the OCS signal, respectively. ω_s and $\omega_{\rm RF}$ are the frequency of the optical carrier and the RF signal, respectively. Then, the OCS signal is detected by a high-speed photodetector (PD), and the RF component of the output current from the PD is proportional to

$$i_{\rm AC}(t) \propto 2R(A_{-1}A_1)\cos[2\omega_{\rm RF}t] \tag{4}$$

where R is the responsivity of the PD. The implementation of photonic RF phase shifter requires a phase difference between the two tones of the OCS signal. This can be achieved by changing the resonance of the microring. When a pump light is fed into the microring resonator, the absorbed energy is eventually converted to the thermal energy and results in the thermal nonlinear effect, which causes a red shift of the resonance [9]. As the thermooptic coefficient is very large in silicon, the phase shift of the signal can be tuned by controlling the pump light power with a low value. Therefore, the OCS signal is optically processed to change the two tones by a factor of $A'_{-1}\exp(j\theta_{-1})$ and $A'_1\exp(j\theta_1)$, respectively. Here, $A'_{\pm1}$ and $\theta_{\pm1}$ represent the amplitude gain and the optical phase shift, respectively. The two tones of the OCS signal experience different phase shift and the optical field of the OCS signal becomes

$$E_{\rm out}(t) = A_{-1}A'_{-1}\exp[j(\omega_s - \omega_{\rm RF})t]\cdot\exp(j\theta_{-1}) + A_1A'_1\exp[j(\omega_s + \omega_{\rm RF})t]\cdot\exp(j\theta_1). \tag{5}$$

After PD detection, the RF component is

$$i'_{\rm AC}(t) \propto 2R(A_{-1}A_1)(A'_{-1}A'_1)\cos[2\omega_{\rm RF}t + (\theta_{-1} - \theta_1)]. \tag{6}$$

Compared with (4), (6) shows that the induced optical phase shift from the two tones of the OCS signal has been completely transferred to the RF signal. If one tone of the OCS signal is controlled off resonance, a maximum tunable range of 2π-rad phase shifting for the OCS signal can be obtained by sweeping the other tone across the resonance.

III. Experimental Setup and Results

In this experiment, a 20-μm-radius silicon microring resonator is used, which is fabricated on a silicon-on insulator (SOI) wafer with a 250-nm-thick silicon slab on top of a 3-μm silica buffer layer. The cross section of the silicon waveguide is 450 × 250 nm with a mode area of about 0.1 μm^2 for transverse-electric (TE) optical mode in such a high-index-contrast

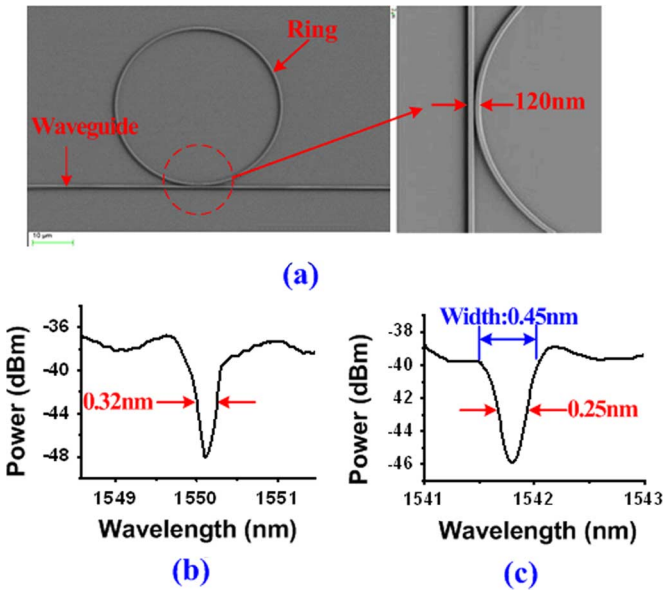

Fig. 2. (a) SEM photo of the microring resonator. (b) Spectrum of the device at 1550.1 nm. (c) Spectrum of the device at 1541.8 nm.

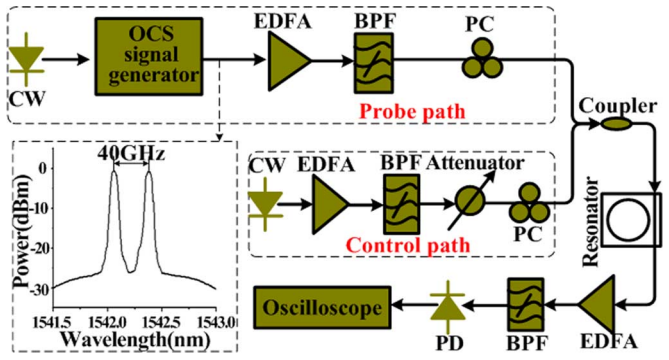

Fig. 3. Experimental setup for the proposed photonic RF phase shifter. CW: continuous wave; EDFA: erbium-doped fiber amplifier; BPF: bandpass filter; PC: polarization controller: and PD: photo-detector.

structure. The microring is side-coupled to a straight waveguide with an air gap of 120 nm between the straight waveguide and the microring. At each end of the straight silicon waveguide, there is a gold grating coupler to couple the light near-vertically from single mode fibers [10], and the measured fiber-to-fiber loss is ~20 dB. Fig. 2(a) shows the scanning electron microscope (SEM) photo of the silicon microring resonator. To facilitate the coupling of the control light into the ring, we set the control light at a 1550.1-nm resonance, which has a ~14-dB notch depth and a ~0.32-nm 3-dB bandwidth, as shown in Fig. 2(b). The resonance wavelength of the probe path is 1541.8 nm, with an 8-dB notch depth and a 3-dB bandwidth of ~0.25 nm. Its spectral response is shown in Fig. 2(c). Fig. 3 illustrates the experimental setup of the proposed scheme. An OCS signal with a 40-GHz frequency spacing is obtained from a signal generator with the optical spectrum indicated in inset of Fig. 3. In the experiment, the two sidebands of the 40-GHz OCS signal are located at the right side of the resonance. The central wavelength of the 40-GHz signal is set at 1542.2 nm to obtain maximum phase difference between the two sidebands

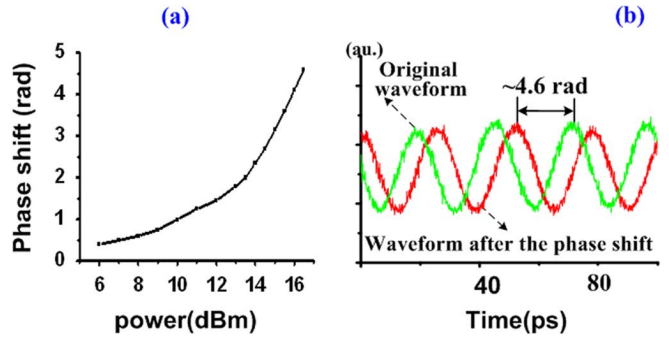

Fig. 4. (a) Phase shifter verses the pump power. (b) Waveforms before and after the phase shift.

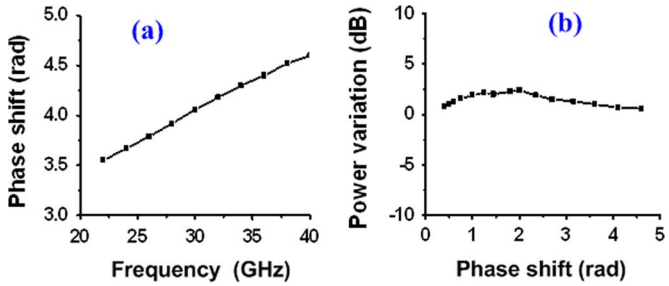

Fig. 5. (a) Maximum phase shift versus RF frequency. (b) Power variation as function of the phase shift.

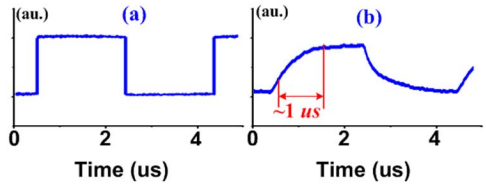

Fig. 6. (a) Waveform of the original baseband data. (b) Waveform of the down-converted data.

when red shift of the resonator happens. The pump light is amplified by a high-power erbium-doped fiber amplifier (EDFA) followed by an attenuator to adjust the pump power. The pump light and the probe signal are coupled through a 3-dB coupler to the microring resonator by the vertical coupling system. The output signal of the microring resonator is amplified using an EDFA, and a bandpass filter (BPF) is used to separate the probe signal, which is injected into a 40-GHz PD for detection. An oscilloscope is used to record the waveforms and observe the phase shifts. As the gold grating coupler of the microring is polarization dependent, two polarization controllers (PCs) are inserted before the coupler to ensure the probe signal and the control light are in TE mode.

We first measure the phase shift versus the optical power of the pump light, as shown in Fig. 4(a), where the maximum phase shift is ~4.6 rad. The required power to obtain the maximum phase shift is ~16.5 dBm, measured at the input fiber to the silicon microring (~6.5 dBm into the ring). For the maximum phase shift of ~4.6 rad, the signal waveform is still well preserved, as shown in Fig. 4(b), verifying the feasibility of constructing a tunable photonic RF shifter based on the silicon microring resonator. We test the RF frequency response of the photonic phase shifter at the maximum phase shift, as shown in Fig. 5(a). For the microring we employed, the frequency spacing of the two tones is smaller than the width of the resonance [see Fig. 2(c)], which results in less than 2 π relative phase shift difference between the two tones. Therefore, the desired maximum phase shift of 2π rad cannot be obtained. This limitation can be resolved by a microring with a narrower resonance. Finally, Fig. 5(b) depicts the dependence of the amplitude variation on the phase shift. Less than 3-dB power variation is observed which mainly results from the loss of the tones located at the resonance region. The RF power fluctuation can be minimized by reducing the loss of the microring and optimizing the coupling to achieve a desired all-pass filtering characteristic.

The response speed of the phase shift is also experimentally verified. The control light was modulated by a 500-kb/s baseband data with its waveform provided in Fig. 6(a). Based on the thermooptic effect in the ring resonator, the probe signal is phase modulated by the 500-kb/s data. After PD detection, the phase-modulated probe signal is converted to an electrical signal, which is further down-converted by mixing with a local oscillator (LO) signal and then passes through a low-pass filter to obtain the baseband signal, as shown in Fig. 6(b). The phase-modulated probe signal is thus converted to an intensity signal, and the rise time of the intensity signal represents the respond speed of the phase shift. Fig. 6(b) shows the rise time is ~1 μs, which is consistent with the theory and limited by the thermal dissipation time of silicon [9].

IV. Conclusion

In summary, we have demonstrated a tunable photonic RF phase shifter using thermal nonlinear effect in a silicon-based microring resonator. It provides a wide operation bandwidth with compact size. The prototype device achieved a phase-shift tuning range of 0-4.6 rad for the 40-GHz signal.

References

[1] K. Ghorbani, A. Mitchell, R. B. Waterhouse, and M. W. Austin, "A novel wide-band tunable RF phase shifter using a variable optical directional coupler," *IEEE Trans. Microw. Theory Tech.*, vol. 47, no. 5, pp. 645–648, May 1999.

[2] M. R. Fisher and S. L. Chuang, "A microwave photonic phase-shifter based on wavelength conversion in a DFB laser," *IEEE Photon. Technol. Lett.*, vol. 18, no. 16, pp. 1714–1716, Aug. 15, 2006.

[3] A. Loayssa and F. J. Lahoz, "Broad-band RF photonic phase shifter based on stimulated Brillouin scattering and single-sideband modulation," *IEEE Photon. Technol. Lett.*, vol. 18, no. 1, pp. 208–210, Jan. 1, 2006.

[4] J. Han *et al.*, "Multiple output photonic RF phase shifter using a novel polymer technology," *IEEE Photon. Technol. Lett.*, vol. 14, no. 4, pp. 531–533, Apr. 2002.

[5] J. F. Coward, T. K. Yee, C. H. Chalfant, and P. H. Chang, "A photonic integrated-optic RF phase-shifter for phased-array antenna beam-forming applications," *J. Lightw. Technol.*, vol. 11, no. 12, pp. 2201–2205, Dec. 1993.

[6] Q. Li, Q. Chang, F. Liu, Z. Zhang, M. Qiu, and Y. Su, "Optical tunable microwave-photonic phase shifter based on silicon microring resonator," in *Proc. ECOC 2008*, p. 2.12.

[7] S. Blair and K. Zheng, "Intensity-tunable group delay using stimulated Raman scattering in silicon slow-light waveguides," *Opt. Express*, vol. 14, no. 3, pp. 1064–1069, Feb. 2006.

[8] T. Kawanishi, H. Kiuchi, M. Yamada, T. Sakamoto, M. Tsuchiya, J. Amagai, and M. Izutsu, "Quadruple frequency double sideband carrier suppressed modulation using high extinction ratio optical modulators for photonic local oscillators," *Proc. IEEE Microwave Photonics Conf. 2005*, p. PDP-03.

[9] Q. Xu and M. Lipson, "Carrier-induced optical bistability in silicon ring resonators," *Opt. Lett.*, vol. 31, no. 3, pp. 341–343, Feb. 2006.

[10] S. Scheerlinck, J. Schrauwen, F. Van Laere, D. Taillaert, D. Van Thourhout, and R. Baets, "Efficient, broadband and compact metal grating couplers for silicon-on-insulator waveguides," *Opt. Express*, vol. 15, no. 15, pp. 9639–9644, Jul. 2007.